Forest Ecology and Management 310 (2013) 1–9

Contents lists available at ScienceDirect

Forest Ecology and Management

journal homepage: www.elsevier.com/locate/foreco

Forest performance during two consecutive drought periods: Diverging long-term trends and short-term responses along a climatic gradient

Michael Dorman [a,*], Tal Svoray [a], Avi Perevolotsky [b], Dimitrios Sarris [c,d,e]

[a] Department of Geography and Environmental Development, Ben-Gurion University of the Negev, Beer-Sheva 84105, Israel
[b] Department of Agronomy and Natural Resources, Agricultural Research Organization, Volcani Ctr, Bet Dagan 50250, Israel
[c] Faculty of Pure & Applied Sciences, Open University of Cyprus, 2252 Latsia, Nicosia, Cyprus
[d] Department of Biological Sciences, University of Cyprus, 1678 Nicosia, Cyprus
[e] Division of Plant Biology, Department of Biology, University of Patras, 265 00 Patras, Greece

ARTICLE INFO

Article history:
Received 25 May 2013
Received in revised form 5 August 2013
Accepted 5 August 2013
Available online 5 September 2013

Keywords:
Drought response
Landsat
Normalized Difference Vegetation Index (NDVI)
Pinus halepensis
Spatial interpolation

ABSTRACT

Forest decline, attributed to increased aridity under global climate change, has been observed with rising frequency worldwide. One of the knowledge gaps making its spatially explicit prediction difficult is the identification of the climatic settings that generate a significant change in the forest state. A relatively rare sequence of unfavourable climatic events – a short extreme drought followed by a prolonged moderate drought within one decade – has allowed us to examine how rainfall amount affects forest performance.

Large-scale monitoring, at high spatial and temporal resolutions, is required to study climatic effects on forest performance. Therefore, time-series of spatially interpolated rainfall maps, remote sensing images and tree growth data were used to estimate the environmental settings to which the forests are exposed, and the corresponding forest performance responses. Performance was estimated from Normalized Difference Vegetation Index (NDVI) values obtained from 32 Landsat satellite images for 1994–2011. To widen the study perspective we sampled forest performance along a rainfall gradient (250–750 mm) in the planted *Pinus halepensis* forests in Israel.

Performance response was not spatially homogeneous. Three response types could be identified along the rainfall gradient: stable performance with low correlation to rainfall pattern in the humid region (>500 mm), moderate performance decline with high correlation to rainfall in the intermediate region (350–500 mm), and steep performance decline with intermediate correlation to rainfall in the arid region (<350 mm). The response to the second drought differed among regions, unlike the response to the first drought, which was homogeneous.

The observed diverging performance trend along the climatic gradient can be attributed to the varied importance of water availability as a limiting factor. The reduced effect of rainfall on performance deviations, the steep performance decline, and the difference between responses to the first and second droughts at the most arid locations, imply to higher importance of multi-annual accumulated and carried-over drought stress effects at these locations.

1. Introduction

Large-scale forest decline, i.e. defoliation, reduced tree growth rate and increased mortality, attributed to increasing aridity under global climate change, have been observed with rising frequency worldwide (Allen et al., 2010). For example, widespread mortality of *Pinus edulis*, *Pinus ponderosa*, and other species was recorded in south-western USA in 2002–2003, following an extreme drought (Breshears et al., 2005; Shaw et al., 2005). This event was considered an ecosystem "crash" (Breshears et al., 2011; Breshears and Allen, 2002), since in semiarid environments it can take more than a century for tree cover to fully re-establish. The magnitude of these ecosystem functional changes, generated by forest mortality, could be revealed by remote sensing with multispectral sensors (Breshears et al., 2005; Huang et al., 2010; Rich et al., 2008; Yuhas and Scuderi, 2009).

The increased forest mortality raises concerns regarding the fate of forest cover and sustainability of stands if climate becomes drier. However, forest decline and mortality are not well understood processes, either on the individual tree level (McDowell et al., 2011) or on the whole-forest level (Allen et al., 2010). In particular, it is asserted that the link between forest decline and causal

* Corresponding author. Tel.: +972 86479054.
E-mail address: michael.dorman@mail.huji.ac.il (M. Dorman).

0378-1127/$ - see front matter © 2013 Elsevier B.V. All rights reserved.
http://dx.doi.org/10.1016/j.foreco.2013.08.009

climatic drivers should be systematically examined to evaluate forest sensitivity to climatic changes in various environmental settings (Allen et al., 2010).

In water-limited ecosystems, decline in forest performance is generally expected to be greater at the arid edge of a species distribution, where water availability constraint on vegetation is highest (Allen et al., 2010; Babst et al., 2013; Linares et al., 2009). However, studies of forests arid distribution limits received smaller amount of attention among forest-related ecological studies until now (Hampe and Petit, 2005; Matyas, 2010; but see Vicente-Serrano, 2007). For example, Carnicer et al. (2011) studied crown defoliation rates in European forests. The authors have found that a significant increase in defoliation rates occurred during 1987–2007 only in southern Europe, in contrast to the stable state observed in northern and central Europe over the same period. A divergent trend between the arid forest border and more humid locations with *Pinus halepensis* forests was also recently reported from Spain (Vicente-Serrano et al., 2010c).

Both abovementioned studies (Carnicer et al., 2011; Vicente-Serrano et al., 2010c) examined long-term performance trends with respect to the location along climatic gradients (i.e., average rainfall amount), but not to the temporally explicit trajectory of annual rainfall at each location. However, the way in which climatic events, such as droughts, translate into short-term deviations of forest performance from their long-term trend holds information on forest resilience when facing climatic deviations. For example, a significant long-term trend may indicate steady growth in areas which are not water-limited (in the case of a positive trend) or steady decline in locations irreversibly damaged by drought (in the case of a negative trend). No significant long-term performance changes, accompanied by short-term deviations of performance in response to rainfall amount variation, however, may indicate limits of a species distribution. Those are the locations where the role of rainfall as a limiting factor to performance is strongest, although no pronounced growth or decline has yet been observed. Drying trends have been observed around the Mediterranean (e.g. Kafle and Bruins, 2009; Sarris et al., 2007), while global climate change models predict further desertification in the region (Giorgi and Lionello, 2008). Therefore, it is particularly important to acknowledge how sequences of climatic deviations, such as recurrent drought, affect forest performance (Girard et al., 2012; Sanchez-Salguero et al., 2012; Sarris et al., 2011).

In forest science, remote sensing is a modern and efficient tool to obtain high temporal and spatial resolution data on vegetation performance and physiology (Pettorelli et al., 2005; Zhu et al., 2012). Indices summarizing reflectance patterns obtained from multispectral sensors (such as TM and ETM+ on Landsat satellites) were developed for these purposes. The most commonly used index in ecological studies, the Normalized Difference Vegetation Index (NDVI) (Rouse et al., 1973; Tucker, 1979), is used to quantify green biomass (Pettorelli et al., 2005; Wang et al., 2011). NDVI was used to assess forest structural and physiological responses to climatic change in numerous studies, including studies on *P. halepensis* forests (Lloret et al., 2007; Vicente-Serrano et al., 2010c; Volcani et al., 2005) as well as on forests in other ecosystems (Verbyla, 2008). In the present study, NDVI is a measure of forest performance, reflecting green biomass quantity and state (Pettorelli et al., 2005; Wang et al., 2011), of the forested area in a given location, at a given year.

P. halepensis grows naturally in the Mediterranean region, mainly in the western part but a few isolated populations have been located in the eastern part, including Israel (Schiller, 2000). Its natural distribution is limited by minimum annual precipitation of 450 mm (Liphschitz and Biger, 2001; Schiller, 2000). However *P. halepensis* was planted under a wide range of climatic conditions in Israel, including regions with annual rainfall ranging between 200 and 850 mm, thus extending beyond the climatic envelope of the species' natural distribution. Planted forests cover about 8% of the Mediterranean climatic zone in Israel (Osem et al., 2008) and are dominated (~75%) by conifers, of which *P. halepensis* is the most common species (Perevolotsky and Sheffer, 2009). The majority of the forests are monocultures of even-aged trees (Osem et al., 2009), planted during a relatively short time period (1961–1970; Israel Forest Service GIS layer, 2011).

Recently, increased mortality of *P. halepensis* in the planted forests of Israel was reported in the southernmost locations (Schiller et al., 2005, 2009; Ungar et al., 2013), following a sequence of two drought periods: a short extreme drought (1998–2000) and a prolonged moderate drought (2005–2011). This has provided a unique opportunity to examine forest performance response to recurrent drought events.

In the present study we examine the response of *P. halepensis* forests planted along a rainfall gradient of 250–750 mm in Israel, to two consecutive drought periods during 1994–2011, as related to annual rainfall amount.

The principal questions that this study aims to tackle are:

1. How did forest performance response to two consecutive drought periods vary along a wide rainfall gradient, extending from the arid forest border towards the more humid Mediterranean zone?
2. Did the response to a second drought period differ from that of the first drought period, and how did this difference vary along the rainfall gradient?

2. Materials and methods

2.1. Study area

The study area encompasses 46 forests (see Figs. S1 and S2 in Supporting information) located in central and northern Israel, amounting to a total sampled area of 31.7 km^2. The forests are spread across a climatic gradient extending from semi-arid to Mediterranean conditions, i.e., annual rainfall ranging from 236 to 746 mm. The climate in the region is characterized by winter rains occurring mainly between December and March, and a relatively long, dry, hot summer (Osem et al., 2009).

Three forests along the rainfall gradient were chosen for dendrochronological sampling (Fig. S2). All sites were located on southern aspects and were of comparable age (planting year of 1969, 1965 and 1960 for the arid, intermediate and humid sites, respectively). Since growth declines with age (Sarris et al., 2007, 2011), the slight age increase towards the humid edge of the gradient in fact makes the comparison more conservative. The sites are hereafter referred to as "arid site", "intermediate site" and "humid site". Note that we do not refer to climatic regions; these labels are used to enable easier reference to relative position along the rainfall gradient (the same applies when referring to "arid", "intermediate" and "humid" parts of the rainfall gradient, see below).

2.2. Remote sensing data

To estimate forest structural responses on a large spatial scale, 30 Landsat-5 TM and 2 Landsat-7 ETM+ images from the period 1994–2011 were used. Two adjacent Landsat scenes (path 174, rows 37 and 38) from the same date were merged to cover the area of interest; sample sizes were 15 and 17 images for the northern and southern parts of the area, respectively. Images were selected from a relatively short time period during the end of the dry season (8 September–16 October) for two reasons (Vicente-Serrano et al., 2010c). First, during the dry season there is lower variation in

water availability for the trees, therefore there is lower seasonal variation in the vegetation activity signal. Second, herbaceous vegetation is completely dry during the summer; therefore a higher proportion of the spectral signal can be attributed to *P. halepensis* trees.

Images were geometrically corrected in the AutoSync Workstation module of Erdas Imagine 2011 software (ERDAS, 2011), by using a 5th-order polynomial geometric model. The images from 2003 were chosen as the reference set for all other images in the series. Root Mean Square Error (RMSE) was <0.5 pixel length in all cases. Radiometric calibration was performed based on up-to-date coefficients (Chander et al., 2009). Atmospheric correction was applied with the Dark Object Subtraction 4 method (Song et al., 2001). A Dark Object Subtraction method was chosen because supplementary atmospheric data (such as Aerosol Optical Depth) are not available for the older images, which necessitated application of an image-based method. Manually prepared cloud masks were used in order to exclude cloud and cloud shadow areas from the analysis.

The NDVI was calculated as:

$$\mathrm{NDVI} = \frac{\rho_{IR} - \rho_R}{\rho_{IR} + \rho_R} \quad (1)$$

in which ρ_{IR} is the reflectivity in the near-infrared region (Landsat band 4), and ρ_R is the reflectivity in the red region (Landsat band 3) of the electromagnetic spectrum. Image processing, spatial interpolation and statistical analyses were applied by using R software (R Development Core Team, 2012). Atmospheric correction of Landsat images was done with the "landsat" package (Goslee, 2011).

Images were aggregated from 30-m to 90-m resolution by using a mean function, to reduce the amount of data as well as to reduce position errors stemming from geometric correction inaccuracy. A polygonal layer of Israeli planted forests (obtained from the Israeli forest service, KKL) was used to delineate areas within a given forest containing >80% *P. halepensis*. Mean NDVI values time series of each forest was then extracted from 90-m pixels completely within those areas of interest.

2.3. Rainfall data

Annual rainfall grids with 1000-m resolution were produced by applying spatial interpolation to data from 96 meteorological stations (Fig. 1a), for 26 rainfall seasons (1985–2011). Two interpolation methods were evaluated for this task: Ordinary Kriging, and Universal Kriging (Carrera-Hernandez and Gaskin, 2007; Di Piazza et al., 2011; Vicente-Serrano et al., 2003) with all possible combinations of three covariates – elevation (Goovaerts, 2000), distance from the Mediterranean Sea, and latitude. Prediction accuracy was compared by using the mean RMSE obtained from Leave-One-Out cross validation. Universal Kriging with elevation as a covariate yielded the lowest average RMSE (58.2 mm) among the 26 years, therefore this method was chosen for preparing the rainfall maps (Table S1). Since interpolation accuracy decreases with distance, only those forests within 15 km of the nearest meteorological station were considered for analysis. Spatial interpolation of rainfall data was done with the "gstat" package (Pebesma, 2004) in R.

A monthly time series of Standardized Precipitation-Evapotranspiration Index (SPEI; Vicente-Serrano et al., 2010a, 2010b) was obtained (Fig. 1b) in order to provide a broader perspective on the increased aridity in the region within the temporal window that is relevant for the studied planted forests (1960–2011). The SPEI is a site-specific drought indicator of deviations from the average water balance (precipitation minus potential evapotranspiration). Different SPEI time series may be calculated for different time scales, representing the cumulative water balance over the previous n months (Vicente-Serrano et al., 2013). A 12-months integration period was chosen since a stronger response of *P. halepensis* to cumulative droughts over 11-months was detected in a previous study (Pasho et al., 2011). The data were downloaded from the Global SPEI database, available at a 0.5° spatial resolution and monthly time resolution (http://www.sac.csic.es/spei/), for a grid cell located at the center of the studied area (32°15′N, 35°15′E).

2.4. Dendrochronological methods

Sampling took place during autumn 2011–spring 2012. In each of the three sites (Fig. S2), 30 living unsuppressed trees were selected. GPS receiver was used to record the coordinates of all sampled trees. Two wood cores were extracted from opposite sides of each tree at breast height using an increment borer. Cores were sanded using increasingly fine sanding paper until tree rings were clearly visible under a binocular microscope. Tree Ring Width (TRW) was measured to an accuracy of 0.01 mm using a LINTAB 6 measuring device (Rinntech, Heidelberg, Germany). Among the two cores from a given tree, the core having better agreement with the site' mean series was chosen according to the "Gleichläufigkeit", a classical time-series agreement test based on sign test (Eckstein and Bauch, 1969). This step was performed using the TSAP software (Rinntech, Heidelberg, Germany). Its purpose was to remove unrepresentative cores having mechanical damage or growth irregularities while retaining the sample of 30 individual trees. The final 90 TRW series were used in order to calculate the mean and standard error of TRW per site per year (Fig. 4).

2.5. Statistical methods

The research questions were examined by fitting linear regression models to the data, and by using model selection procedures (Johnson and Omland, 2004); presence of a given predictor in the best model was interpreted as support for the hypothesis underlying that predictor (i.e. presence of a performance temporal trend and/or an association between performance and annual rainfall amount, see below). Model selection was based on the small-sample unbiased Akaike Information Criterion (AICc) (Johnson and Omland, 2004), which is a modified version of the Akaike Information Criterion (AIC) (Akaike, 1974) containing an additional bias-correction term for small sample sizes. For simplicity, AICc is hereafter referred to as AIC.

The effect of rainfall on NDVI was evaluated by selecting one of four models: the one described in Eq. (2) and the three simplified nested models each of which lacked one or both of the predictors, t and $Rain_t$.

$$\mathrm{NDVI}_t = \beta_0 + \beta_1 * t + \beta_2 * Rain_t + \varepsilon \quad (2)$$

in which NDVI_t is the value of NDVI in year t, $Rain_t$ is the rainfall amount during the previous year; i.e., NDVI_t is an NDVI value obtained in September–October of year t, and $Rain_t$ is the rainfall amount during the previous wet season, i.e., October–April of years $t-1$ to t, and ε is the error term.

The model-fitting procedure was performed separately for the NDVI time series of each forest. Forests samples included 46 locations (see Fig. S2), which were selected according to three criteria: (1) forest size is at least 10 (90 × 90 m) pixels, i.e., at least 90 Landsat pixels; (2) at least 14 years of observation remaining after removal of years in which more than 10% of the data were missing because of cloudiness; (3) four forests were removed from the analysis because they had experienced fires during the studied period – one known to have occurred in 1995 (Levin and Saaroni, 1999) and three others more recently, as verified by reference to aerial photographs of these locations from 2010.

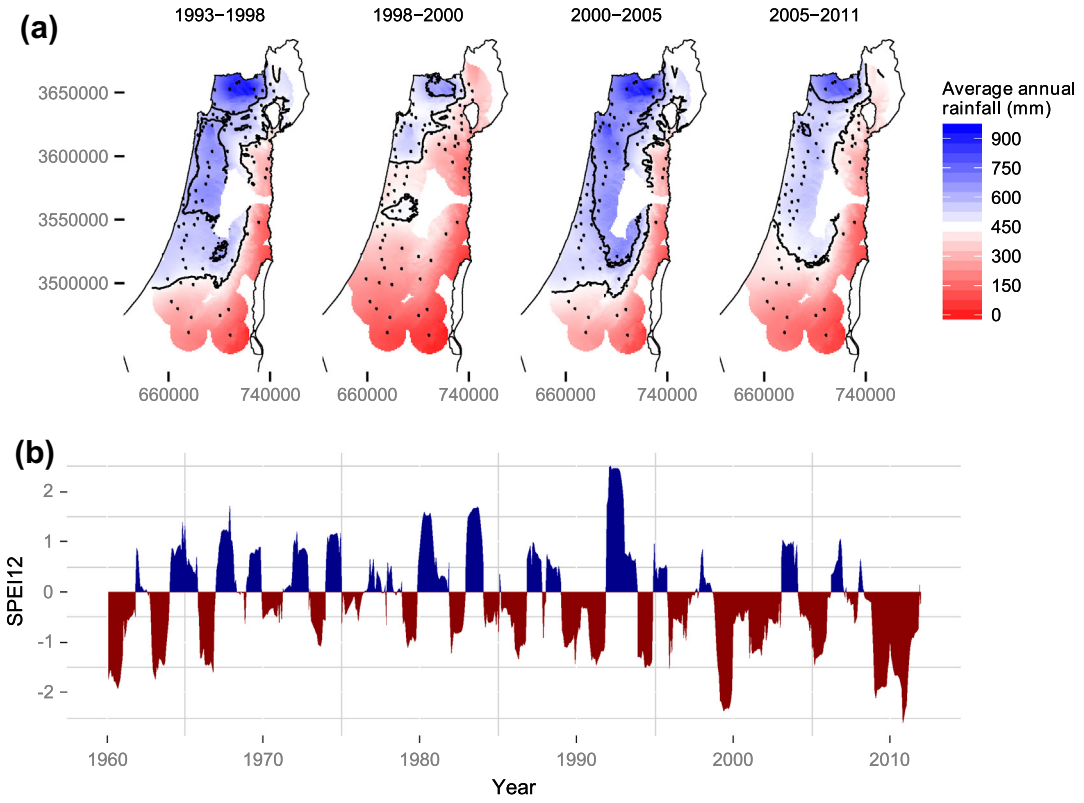

Fig. 1. (a) Maps of average annual rainfall during four consecutive periods: 1993/94–1997/98 (5 rain seasons), 1998/99–1999/00 (2 rain seasons), 2000/01–2004/05 (5 rain seasons) and 2005/06–2010/11 (6 rain seasons). Whereas the first (1993–1998) and third (2000–2005) periods had average rainfall distribution, the second period (1998–2000) encompassed a short but extreme drought and the fourth (2005–2011) – a prolonged moderate drought. Lines show the 450 mm and the 600 mm isohyets. Values were obtained by spatial interpolation of data from 96 meteorological stations (shown as black points) by using Universal Kriging with elevation as a covariate. Universal Transverse Mercator (UTM) zone 36 N coordinates (m) are shown on the axes. (b) A cumulative Standardized Precipitation-Evapotranspiration Index (SPEI) over the previous 12-months period as function of month, during 1960–2011, in the central part of the studied area. The SPEI is a standardized variable; values above zero (blue) denote water surplus, values below zero (red) denote water deficit. (For interpretation of the references to color in this figure legend, the reader is referred to the web version of this article.)

Rainfall amounts for each forest were standardized to mean of zero and standard deviation of 1, according to the 26 years of observation, i.e., standardized anomaly values were calculated (Anderson et al., 2010), to enable comparison among forests (Schielzeth, 2010).

An example of the input data and of the model selection procedure on two of the 46 forests can be found in Fig. S3.

3. Results

Rainfall maps of four consecutive periods between 1993 and 2011 (Fig. 1a) show that the studied period began with five average years (1993–1998). Two extremely dry years followed (1998–2000). The next five years (2000–2005) returned to average conditions, and were followed by six years of moderate drought (2005–2011). The two drought periods (1998–2000 and 2005–2011) represent a relatively rare sequence of unfavourable climatic events. For example, the rainfall record for 1963–2011 at the Bet Dagan station (central Israel; see Fig. S4) shows that the last 14-year period (1998–2011) was particularly dry in that it included 12 below-average rainfall years (all except for 2002 and 2003), including the driest year on the record (1999). The SPEI time series (Fig. 1b) for 1960–2011 also showed that the two recent drought periods (1998–2000 and 2005–2011) encompassed the most extreme conditions the forests have experienced since they were planted.

The temporal trend of NDVI and the effect of rainfall on NDVI were examined at the 46 forest locations. Fitted coefficients of the two terms in Eq. (2) are plotted for each location on a map (Fig. 2a and b) and also on a graph, as functions of average rainfall at the location (Fig. 2d and e). Adjusted R^2 values of the respective models are shown on a map (Fig. 2c) and also on a graph (Fig. 2f).

Fig. 2a shows the temporal trend of NDVI, which is expressed in the fitted values of the coefficient β_1 from Eq. (2). It appears that NDVI decreased in the arid region, while increasing or remaining constant in the humid region (e.g. Fig. S3), even though the whole studied area was affected by drought (Fig. 1a). Fig. 2d shows the NDVI trend from Fig. 2a as a function of the average rainfall in the 46 locations. This allows quantitative assessment of the relation between the temporal trend of NDVI and the average rainfall along the climatic gradient in Israel. The average annual rainfall that yielded an estimated zero trend was 543 mm. In other words, during the examined period, direction and magnitude of the NDVI trend were related to position along the rainfall gradient; the NDVI trend during 1994–2011 was characterized by a transition from decreasing to increasing at 543 mm. Naturally, this pattern led to an increase in NDVI contrast along the rainfall gradient during 1994–2011 (Fig. 3e).

Fig. 2b shows the estimated effects of previous-year rainfall on NDVI at the 46 locations, which is the fitted value of the coefficient β_2 from Eq. (2). The fitted coefficients were positive in all cases where this variable appeared in the lowest AIC model, meaning that effect of previous year rainfall on NDVI was either positive or absent. However, the strength of this relationship differed between the more humid and more arid parts of the studied climatic gradient. Fig. 2e shows the effect of rainfall depicted in Fig. 2b as a function of the average rainfall in the 46 locations; the effect of rainfall on NDVI appears to be stronger in the more arid locations than in the more humid ones. However, unlike the relation between the trend of NDVI and the climatic gradient (Fig. 2d), the

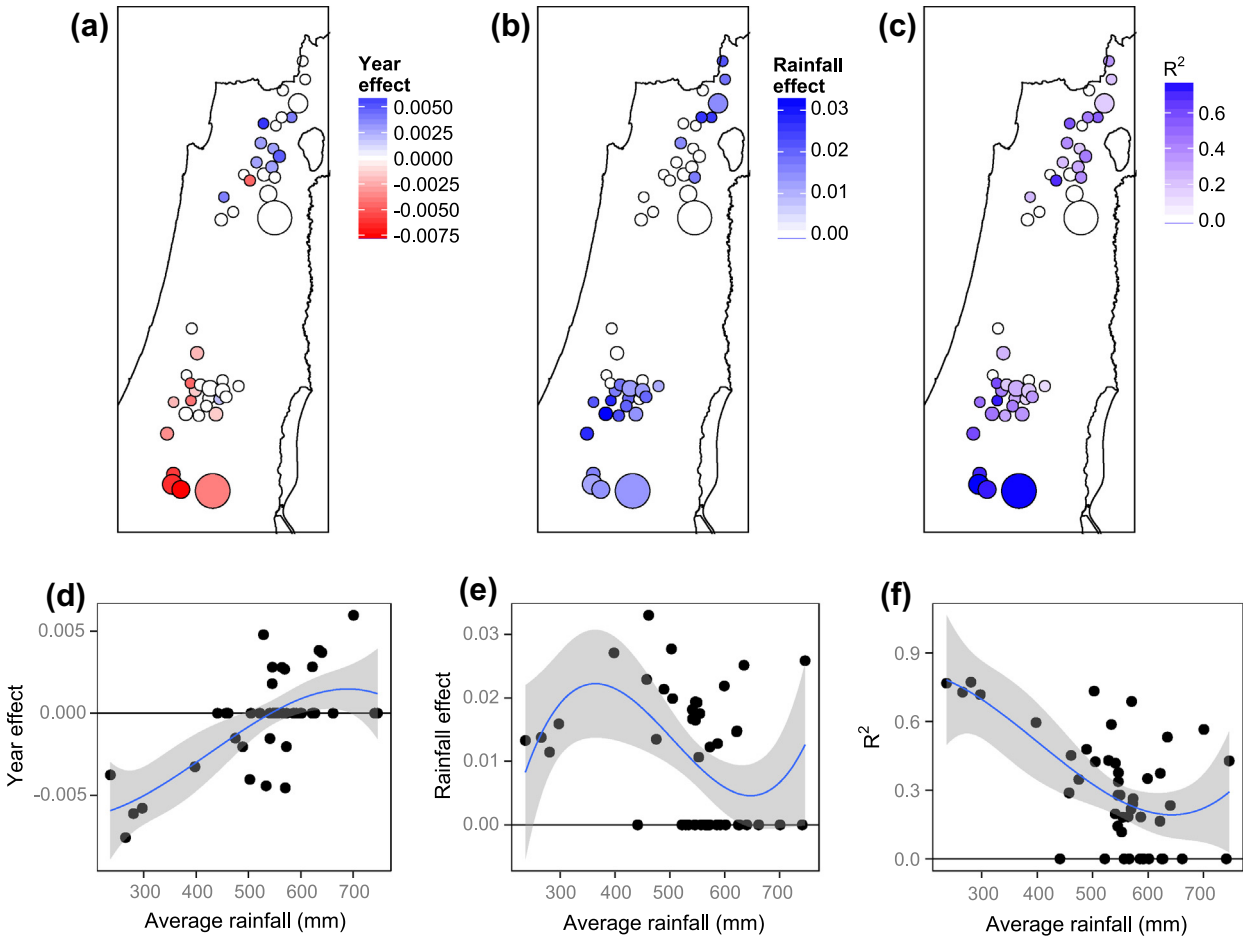

Fig. 2. Maps of the coefficients and adjusted R^2 from the lowest AIC Linear models describing NDVI as function of year and of rainfall in 46 forests in Israel (Eq. (2)): (a and d) – Year effect β_1, (b and e) – Rainfall effect β_2, and (c and f) – Adjusted R^2. Coefficient values are shown in geographical space (a–c) and as functions of average rainfall at the location (d–f). Third-order polynomial regression-fitted lines with 95% confidence interval are shown (d–f); all were significant – (d) $p < 0.001$ and adjusted $R^2 = 0.43$, (e) $p < 0.05$ and adjusted $R^2 = 0.13$, (f) $p < 0.001$ and adjusted $R^2 = 0.34$. Average rainfall values are based on the period 1985–2011. Symbol size in (a–c) is proportional to forest size, ranging between 11 and 656 pixels of (90 × 90) m. (For interpretation of the references to color in this figure legend, the reader is referred to the web version of this article.)

relation between the effect of rainfall and the climatic gradient seems distinctly non-linear (Fig. 2e). The effect of annual rainfall on NDVI was strongest around 400 mm, and decreased towards the arid forest border (below 350 mm) as well as towards the humid region (above 500 mm; Fig. 2e).

Fig. 2c shows adjusted R^2 values of the fitted models at each location. A higher proportion of NDVI variation is attributed to trend and rainfall effects at the arid region (up to R^2 of 0.77 in both of the largest forests in that region, Fig. 2c), than towards the humid region, where the strength of this relationship gradually decreases (Fig. 2f). Locations with $R^2 = 0$ begin to appear at 440 mm annual rainfall, but become common above 500 mm. At these locations the lowest AIC model did not include any terms except for the intercept, indicating that NDVI was relatively stable in the long-term and not affected by annual rainfall in the short-term.

Fig. 3 summarizes the NDVI change (ΔNDVI) between the beginning and end of each of the four periods defined in Fig. 1a. Instead of evaluating the ΔNDVI (namely $NDVI_{t2} - NDVI_{t1}$) values in each of 46 forests, the $NDVI_{t1}$ and $NDVI_{t2}$ values were plotted as a function of average rainfall, and a smoothing was applied to visualize the "$NDVI_{t1}$ – rainfall" and "$NDVI_{t2}$ – rainfall" relations. The area between the two smoothing lines thus expresses the average ΔNDVI as a function of average rainfall during a given period.

The differing responses of the intermediate and arid (<500 mm) as opposed to humid (>500 mm) parts of the rainfall gradient are apparent. At the arid end, ΔNDVI was negative at all periods except for 2000–2005 (Fig. 3c). However, the increase during 2000–2005 was not sufficient even to compensate for the decrease that occurred during the previous period – 1998–2000 (Fig. 3b) – which was an extreme drought. As a result, the NDVI decrease during 1998–2000, combined with the NDVI decreases of 1994–1998 (Fig. 3a) and 2005–2011 (Fig. 3d), resulted in a negative ΔNDVI for the whole studied period in the more arid region (Fig. 3e).

In the humid region, however, ΔNDVI was negative only during the extreme drought of 1998–2000 (Fig. 3b), and close to zero during the moderate drought of 2005–2011 (Fig. 3d). During the other two periods – 1994–1998 (Fig. 3a) and 2000–2005 (Fig. 3c) – ΔNDVI was positive, resulting in an overall positive ΔNDVI for the humid region for the whole studied period (Fig. 3e).

Another notable feature is that the responses of the two parts of the rainfall gradient to the second moderate drought of 2005–2011 (Fig. 3d) differed, in contrast to their similar responses to the first extreme drought period of 1998–2000 (Fig. 3b). Whereas the responses to the first drought were negative with similar magnitude in both parts (Fig. 3b), the response to the second drought was negative in the arid and intermediate regions but close to zero in the humid region (Fig. 3d).

The three sites where wood cores were sampled differed in their growth patterns (Fig. 4). In an arid site, the lowest TRW value was reached by the end of the second drought, in 2011 (0.22 mm). However, in the intermediate site the lowest TRW was observed during the first drought, in 1999 (0.75 mm), while in 2011 TRW

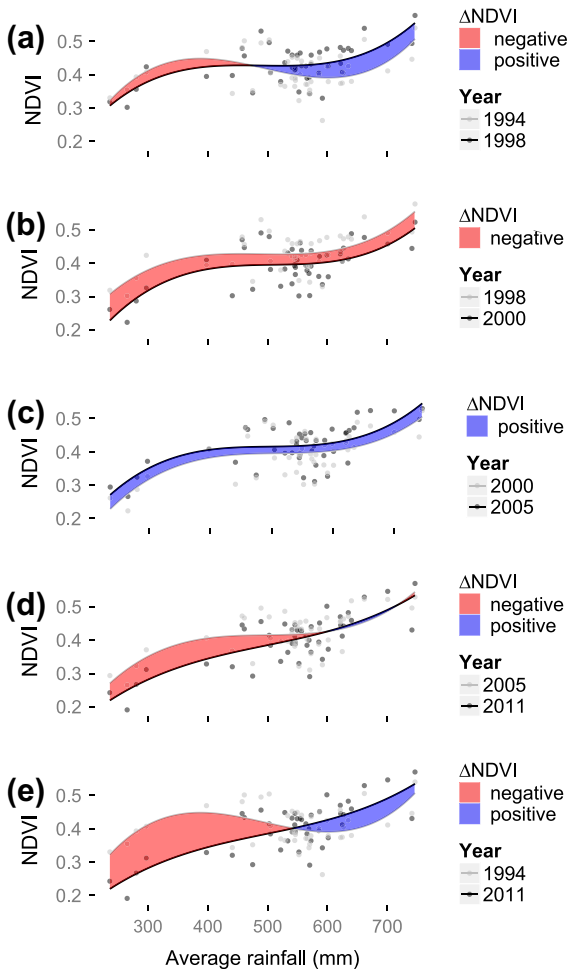

Fig. 3. NDVI differences between beginning and end of four consecutive periods (shown in Fig. 1) and between the beginning and end of the whole studied period, in 46 forests: (a) 1994–1998, (b) 1998–2000, (c) 2000–2005, (d) 2005–2011 and (e) 1994–2011. Third-order polynomial regression-fitted lines are shown – all were significant: $p < 0.01$ and adjusted $R^2 = 0.21$ (1994); $p < 0.001$ and adjusted $R^2 = 0.39$ (1998); $p < 0.001$ and adjusted $R^2 = 0.42$ (2000); $p < 0.001$ and adjusted $R^2 = 0.42$ (2005); $p < 0.001$ and adjusted $R^2 = 0.57$ (2011). Positive and negative differences between fitted lines are filled with blue and red colors, respectively. (For interpretation of the references to color in this figure legend, the reader is referred to the web version of this article.)

was higher (1.09 mm). In the humid site neither the 1999 nor 2011 TRW were particularly low (1.74 and 1.59 mm, respectively), while the lowest TRW was observed in 1992 (1.22 mm).

4. Discussion

The contrasting long-term trend of NDVI along a rainfall gradient in planted *P. halepensis* forests (Fig. 2a and d) may be attributed to the effects of water availability decrease on tree growth under differing water balance conditions. The effect of drought may be stronger in more arid regions, where the forest is more strongly dependent on water availability and weaker in humid regions, which are less water-limited. Evidence for such a divergent trend of *P. halepensis* performance was recently recorded in a few studies, which covered smaller ranges of rainfall variation than those in the present study. Vicente-Serrano et al. (2010c) found a divergent NDVI trend in *P. halepensis* forests in Spain between 391 and 626 mm of annual rainfall; Schiller et al. (2005) and Sanchez-Salguero et al. (2010) demonstrated *P. halepensis* performance decline at locations closer to its arid range limit; Vila et al. (2008) and Linares et al. (2011) reported performance improvement at more humid locations. These findings suggest a decline in performance at the arid forest limit coupled with a performance improvement at the humid part of the gradient. Our results – increasing difference in NDVI along the rainfall gradient (Fig. 3e) – also support this conclusion. This phenomenon is probably related to relative dryness that occurred in the Mediterranean region during the last several decades.

The observed increasing contrast in performance expresses a northward shift of the optimal habitat for a planted *P. halepensis* forest. In the arid part of the gradient, NDVI values decreased, reflecting decrease in green biomass, which may be caused either by increased tree mortality (Schiller et al., 2005, 2009; Ungar et al., 2013) or by defoliation. The latter, too, may eventually lead to increased mortality, since defoliation is detrimental to the trees' carbon budget (Galiano et al., 2011; Girard et al., 2012). We therefore hypothesize that the observed pattern reflects increased defoliation and tree mortality rates in the arid part of *P. halepensis* forests in Israel. Our own field observations as well as observations of others (regional foresters, pers. comm.) give the impression that both drought periods were accompanied by episodes of increased mortality, especially towards the arid forest border. It seems that the present planted *P. halepensis* forests in the semi-arid regions of Israel are not fully adapted to withstand climatic deviations such as the sequence of two consecutive drought periods experienced during 1993–2011 (Fig. 1).

In addition to the divergent performance trend, the two regions (intermediate and arid compared to humid) differed in their responses to the second drought period, which was characterized by a negative trend in NDVI in the arid and intermediate regions and a stable state in the humid region (Fig. 3d). This contrasts with the responses to the first drought period, when all forests responded negatively (Fig. 3b). Two hypotheses may be offered to explain this difference. First, the second drought was relatively moderate (Fig. 1a), therefore, unlike the first extreme drought, rainfall may still have been sufficient to maintain a stable quantity of green biomass in the humid region, even though growth was halted – hence, the zero ΔNDVI (Fig. 3d). In the dry region, however, water availability may already have been low enough to induce drought damage such as defoliation, lower leaf production and tree mortality – hence the negative ΔNDVI (Fig. 3d).

The second hypothesis is related to the recovery from the damage caused by the first, extreme drought (Fig. 3b). This recovery could be quicker in the humid region, since both soil water storage and tree physiological status were probably not as close to limiting levels as in the arid region. However, in the arid region, the drought stress experienced during 1998–2000 could have led to vulnerable physiological state so that many of the trees had not yet recovered by 2005, and therefore exhibited greater and more apparent drought damage during the second drought period of 2005–2011.

Lagging responses to drought were previously observed, for example, in the Rocky Mountains of northern Colorado (USA), where following an early-season drought event, mortality risk of *Picea engelmannii* increased over the subsequent 5 years and mortality risk of *Abies lasiocarpa* increased over the subsequent 11 years (Bigler et al., 2007). "Memory effects" (Schwinning et al., 2004) were previously observed in many water-limited ecosystems (Potts et al., 2006; Richard et al., 2008; Sarris et al., 2007). We hypothesize that critical physiological thresholds of *P. halepensis* were passed (Girard et al., 2012) in the dry region during the extreme drought of 1998–2000, and the resulting damage was carried over to the moderate drought of 2005–2011, and added to the higher impact of drought in the arid region.

Dendrochronological analysis of three sites along the rainfall gradient revealed a pattern that matches our remote sensing findings (Fig. 4). In the arid site the second drought led to very limited

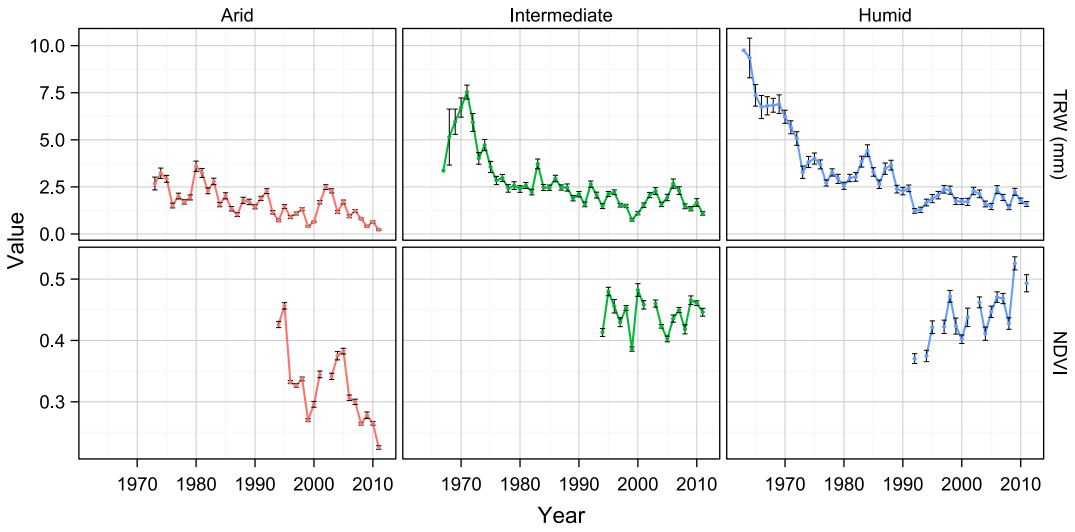

Fig. 4. Tree Ring Width (TRW; upper panel) and NDVI (lower panel) values as function of year, obtained for three sites along the rainfall gradient. Average values ± one standard error are shown for both TRW ($n = 30$ trees for each site) and for NDVI ($n = 10$, 11 and 11 pixels of (30 × 30) m for the arid, intermediate and humid sites, respectively).

growth in 2011. In the intermediate site the narrowest tree-rings were found during the first drought, while the second drought effect was smaller. In the humid site both droughts did not have a noticeable effect on tree growth. In fact, the lowest TRW in the humid site was observed in 1992, which was an unusually wet and cold year, probably due to growth inhibition under low temperatures or snow damage (while growth increased in the arid and intermediate sites in that year, likely due to high water availability). Dendrochronological data provides further evidence for the diverging performance trend along the rainfall gradient. In addition, the fact that in the arid site the lowest TRW value was reached in the last year of the second drought supports the hypothesis of accumulated drought damage.

We hypothesize that the non-linear pattern (Fig. 2e) of performance deviations as related to annual rainfall may be attributed to the interplay between the threshold of climatic limitation on forest performance and the degree of temporal autocorrelation of performance. An analogous framework was previously offered to explain tree-ring width variation among trees in a given site (Fritts et al., 1965); it encompasses two complementary hypotheses. First, the correlation between resource availability, e.g., soil moisture, as determined mainly by rainfall amount, and tree performance, e.g., tree-ring width, becomes stronger as the resource becomes more limiting to the physiological processes of the tree. Thus, in progressing from humid locations towards arid locations, the sensitivity of forest performance to rainfall increases (Fritts et al., 1965). For example, Knutson and Pyke (2008) show that correlations between *Juniperus occidentalis* and *P. ponderosa* growth with climate were stronger at low-elevation (drier) sites than at high-elevation sites in southern Oregon, USA.

The second hypothesis suggests that a decrease in sensitivity of performance to rainfall at the most arid locations could result from increasing temporal autocorrelation at those extreme locations (Fritts et al., 1965) because trees may rely on soil water that accumulated during longer periods than one year (Sarris et al., 2007). In other words, the correlation with previous-year rainfall may weaken because tree performance becomes influenced by a sequence of past rainy seasons and not only by the most recent one.

Taken together, the long-term performance trends (Fig. 2a and d) and the short-term performance deviations correlation with rainfall (Fig. 2b and e) help to identify three zones, characterized by differing responses of *P. halepensis* forests to climate. The arid zone (<350 mm) was characterized by the most negative long-term performance trend, and performance deviations were moderately correlated with rainfall. We hypothesize that this area experienced severe drought damage, which was also carried over to subsequent years, causing a declining pattern of performance and lower responsiveness to annual rainfall amount. It may be expected that additional drought periods in the near future will lead to further mortality and decline in those forests.

The intermediate zone (350–500 mm) was characterized by moderate to zero performance declines, along with high correlation of short-term performance deviations with annual rainfall. We hypothesize that this area currently contains the limit to sustainable distribution of planted *P. halepensis* forests, because it showed only moderate decline during the whole study period, and because its higher correlation between performance deviations and annual rainfall suggests increased resilience in face of climatic deviations. In this case a recovery during the years following drought may be expected.

The humid zone (>500 mm) was characterized by a trend of moderately increasing performance along with a small effect of rainfall on short-term performance deviations. We hypothesize that this area is where the role of water availability as a limiting factor to *P. halepensis* becomes weaker (Zavala et al., 2000). It may be therefore expected that these forests will not be severely affected by future drought periods of the same magnitude as experienced during 1994–2011.

The present study, using remotely sensed NDVI and precipitation records interpolation, enabled considering a broad spatial extent while still working within a single system (i.e. single-species planted forests) along a climatic gradient. The spatio-temporal data on coupled forest performance and rainfall amount trajectories was transformed into continuous descriptors depicting forest performance trends and sensitivity to rainfall amount, thus allowing identification of thresholds in a non-linear system. The observed diverging performance trend in *P. halepensis* along the climatic gradient (i.e. stable performance at the humid end vs. steep decline at the arid edge) may be attributed to the varied importance of water availability as a limiting factor. Moreover, in the most arid region (<350 mm), reduced effect of rainfall on performance deviations, steep performance decline, and differing responses to the first and second droughts were detected. It is proposed that the latter phenomena imply higher importance of

multi-annual accumulated and carried-over drought stress effects at these extreme locations. The present approach may be beneficial in both management-monitoring (e.g. identifying forests deviating from the general climate-performance relation) and scientific aspects of forest and climatic change research (e.g. studying the spatial pattern of climate-performance relation and its environmental determinants).

Acknowledgements

We thank David Brand, Israel Tauber, Ronen Talmor, Efrat Sheffer and Shmuel Sprintsin for providing helpful information and Resources. The Israeli Forest Service (KKL) willingly provided forests GIS layers and purchased the equipment and software for the dendrochronological analysis. We thank Talia Horovitz and the Israel Meteorological Service for providing the rainfall data. We thank Arnon Cooper, Or Livni, Adam Wattenberg and Yoni Waitz for assistance in field work. This study is supported by a grant from the Chief Scientist of the Israeli Ministry of Agriculture and Rural Development and the Jewish National Fund.

Appendix A. Supplementary material

Supplementary data associated with this article can be found, in the online version, at http://dx.doi.org/10.1016/j.foreco.2013.08.009.

References

Akaike, H., 1974. A new look at the statistical model identification. IEEE Trans. Autom. Control AC19, 716–723.
Allen, C.D., Macalady, A.K., Chenchouni, H., Bachelet, D., McDowell, N., Vennetier, M., Kitzberger, T., Rigling, A., Breshears, D.D., Hogg, E.H., Gonzalez, P., Fensham, R., Zhang, Z., Castro, J., Demidova, N., Lim, J.H., Allard, G., Running, S.W., Semerci, A., Cobb, N., 2010. A global overview of drought and heat-induced tree mortality reveals emerging climate change risks for forests. For. Ecol. Manage. 259, 660–684.
Anderson, L.O., Malhi, Y., Aragao, L.E.O.C., Ladle, R., Arai, E., Barbier, N., Phillips, O., 2010. Remote sensing detection of droughts in Amazonian forest canopies. New Phytol. 187, 733–750.
Babst, F., Poulter, B., Trouet, V., Tan, K., Neuwirth, B., Wilson, R., Carrer, M., Grabner, M., Tegel, W., Levanic, T., 2013. Site-and species-specific responses of forest growth to climate across the European continent. Glob. Ecol. Biogeogr. 22, 706–717.
Bigler, C., Gavin, D.G., Gunning, C., Veblen, T.T., 2007. Drought induces lagged tree mortality in a subalpine forest in the Rocky Mountains. Oikos 116, 1983–1994.
Breshears, D.D., Allen, C.D., 2002. The importance of rapid, disturbance-induced losses in carbon management and sequestration. Glob. Ecol. Biogeogr. 11, 1–5.
Breshears, D.D., Cobb, N.S., Rich, P.M., Price, K.P., Allen, C.D., Balice, R.G., Romme, W.H., Kastens, J.H., Floyd, M.L., Belnap, J., Anderson, J.J., Myers, O.B., Meyer, C.W., 2005. Regional vegetation die-off in response to global-change-type drought. Proc. Nat. Acad. Sci. USA 102, 15144–15148.
Breshears, D.D., Lopez-Hoffman, L., Graumlich, L.J., 2011. When ecosystem services crash: preparing for big, fast, patchy climate change. Ambio 40, 256–263.
Carnicer, J., Coll, M., Ninyerola, M., Pons, X., Sanchez, G., Penuelas, J., 2011. Widespread crown condition decline, food web disruption, and amplified tree mortality with increased climate change-type drought. Proc. Nat. Acad. Sci. USA 108, 1474–1478.
Carrera-Hernandez, J.J., Gaskin, S.J., 2007. Spatio temporal analysis of daily precipitation and temperature in the Basin of Mexico. J. Hydrol. 336, 231–249.
Chander, G., Markham, B.L., Helder, D.L., 2009. Summary of current radiometric calibration coefficients for Landsat MSS, TM, ETM+, and EO-1 ALI sensors. Rem. Sens. Environ. 113, 893–903.
Di Piazza, A., Lo Conti, F., Noto, L.V., Viola, F., La Loggia, G., 2011. Comparative analysis of different techniques for spatial interpolation of rainfall data to create a serially complete monthly time series of precipitation for Sicily, Italy. Int. J. Appl. Earth Obs. Geoinf. 13, 396–408.
Eckstein, D., Bauch, J., 1969. Beitrag zur rationalisierung eines dendrochronologischen verfahrens und zur analyse seiner aussagesicherheit. Forstwiss. Centralbl. 88, 230–250.
Fritts, H.C., Smith, D.G., Cardis, J.W., Budelsky, C.A., 1965. Tree-ring characteristics along a vegetation gradient in northern Arizona. Ecology 46, 393–401.
Galiano, L., Martinez-Vilalta, J., Lloret, F., 2011. Carbon reserves and canopy defoliation determine the recovery of Scots pine 4 yr after a drought episode. New Phytol. 190, 750–759.
Giorgi, F., Lionello, P., 2008. Climate change projections for the Mediterranean region. Glob. Planet. Change 63, 90–104.
Girard, F., Vennetier, M., Guibal, F., Corona, C., Ouarmim, S., Herrero, A., 2012. *Pinus halepensis* Mill. crown development and fruiting declined with repeated drought in Mediterranean France. Eur. J. For. Res. 131, 919–931.
Goovaerts, P., 2000. Geostatistical approaches for incorporating elevation into the spatial interpolation of rainfall. J. Hydrol. 228, 113–129.
Goslee, S.C., 2011. Analyzing remote sensing data in R: the landsat package. J. Stat. Softw. 43, 1–25.
Hampe, A., Petit, R.J., 2005. Conserving biodiversity under climate change: the rear edge matters. Ecol. Lett. 8, 461–467.
Huang, C.Y., Asner, G.P., Barger, N.N., Neff, J.C., Floyd, M.L., 2010. Regional aboveground live carbon losses due to drought-induced tree dieback in pinon-juniper ecosystems. Rem. Sens. Environ. 114, 1471–1479.
Johnson, J.B., Omland, K.S., 2004. Model selection in ecology and evolution. Tr. Ecol. Evol. 19, 101–108.
Kafle, H.K., Bruins, H.J., 2009. Climatic trends in Israel 1970–2002: warmer and increasing aridity inland. Clim. Change 96, 63–77.
Knutson, K.C., Pyke, D.A., 2008. Western juniper and ponderosa pine ecotonal climate-growth relationships across landscape gradients in southern Oregon. Can. J. For. Res. – Rev. Can. Rech. For. 38, 3021–3032.
Levin, N., Saaroni, H., 1999. Fire weather in Israel—synoptic climatological analysis. GeoJournal 47, 523–538.
Linares, J.C., Camarero, J.J., Carreira, J.A., 2009. Interacting effects of changes in climate and forest cover on mortality and growth of the southernmost European fir forests. Glob. Ecol. Biogeogr. 18, 485–497.
Linares, J.C., Delgado-Huertas, A., Carreira, J.A., 2011. Climatic trends and different drought adaptive capacity and vulnerability in a mixed *Abies pinsapo–Pinus halepensis* forest. Clim. Change 105, 67–90.
Liphschitz, N., Biger, G., 2001. Past distribution of Aleppo pine (*Pinus halepensis*) in the mountains of Israel (Palestine). Holocene 11, 427–436.
Lloret, F., Lobo, A., Estevan, H., Maisongrande, P., Vayreda, J., Terradas, J., 2007. Woody plant richness and NDVI response to drought events in Catalonian (northeastern Spain) forests. Ecology 88, 2270–2279.
Matyas, C., 2010. Forecasts needed for retreating forests. Nature 464, 1271.
McDowell, N.G., Beerling, D.J., Breshears, D.D., Fisher, R.A., Raffa, K.F., Stitt, M., 2011. The interdependence of mechanisms underlying climate-driven vegetation mortality. Tr. Ecol. Evol. 26, 523–532.
Osem, Y., Ginsberg, P., Tauber, I., Atzmon, N., Perevolotsky, A., 2008. Sustainable management of Mediterranean planted coniferous forests: an Israeli definition. J. For. 106, 38–46.
Osem, Y., Zangy, E., Bney-Moshe, E., Moshe, Y., Karni, N., Nisan, Y., 2009. The potential of transforming simple structured pine plantations into mixed Mediterranean forests through natural regeneration along a rainfall gradient. For. Ecol. Manage. 259, 14–23.
Pasho, E., Camarero, J.J., de Luis, M., Vicente-Serrano, S.M., 2011. Impacts of drought at different time scales on forest growth across a wide climatic gradient in north-eastern Spain. Agric. For. Meteorol. 151, 1800–1811.
Pebesma, E.J., 2004. Multivariable geostatistics in S: the gstat package. Comput. Geosci. 30, 683–691.
Perevolotsky, A., Sheffer, E., 2009. Forest management in Israel – the ecological alternative. Isr. J. Plant Sci. 57, 35–48.
Pettorelli, N., Vik, J.O., Mysterud, A., Gaillard, J.-M., Tucker, C.J., Stenseth, N.C., 2005. Using the satellite-derived NDVI to assess ecological responses to environmental change. Tr. Ecol. Evol. 20, 503–510.
Potts, D.L., Huxman, T.E., Cable, J.M., English, N.B., Ignace, D.D., Eilts, J.A., Mason, M.J., Weltzin, J.F., Williams, D.G., 2006. Antecedent moisture and seasonal precipitation influence the response of canopy-scale carbon and water exchange to rainfall pulses in a semi-arid grassland. New Phytol. 170, 849–860.
R Development Core Team, 2012. R: A language and environment for statistical computing. In: R Foundation for Statistical Computing, Vienna, Austria. ISBN 3-900051-07-0, <http://www.R-project.org/>.
Rich, P.M., Breshears, D.D., White, A.B., 2008. Phenology of mixed woody-herbaceous ecosystems following extreme events: net and differential responses. Ecology 89, 342–352.
Richard, Y., Martiny, N., Fauchereau, N., Reason, C., Rouault, M., Vigaud, N., Tracol, Y., 2008. Interannual memory effects for spring NDVI in semi-arid South Africa. Geophys. Res. Lett. 35, 1–6.
Rouse, J.W., Haas, R.H., Schell, J.A., Deering, D.W. 1973. Monitoring vegetation systems in the Great Plains with ERTS. In: 3rd ERTS Symposium, NASA SP-351 I, pp. 309–317.
Sanchez-Salguero, R., Navarro-Cerrillo, R.M., Camarero, J.J., Fernandez-Concio, A., 2010. Drought-induced growth decline of Aleppo and maritime pine forests in south-eastern Spain. For. Syst. 19, 458–469.
Sanchez-Salguero, R., Navarro-Cerrillo, R.M., Julio Camarero, J.J., Fernandez-Cancio, A., 2012. Selective drought-induced decline of pine species in southeastern Spain. Clim. Change 113, 767–785.
Sarris, D., Christodoulakis, D., Korner, C., 2007. Recent decline in precipitation and tree growth in the eastern Mediterranean. Glob. Change Biol. 13, 1187–1200.
Sarris, D., Christodoulakis, D., Korner, C., 2011. Impact of recent climatic change on growth of low elevation eastern Mediterranean forest trees. Clim. Change 106, 203–223.
Schielzeth, H., 2010. Simple means to improve the interpretability of regression coefficients. Meth. Ecol. Evol. 1, 103–113.
Schiller, G., 2000. Ecophysiology of *Pinus halepensis* Mill. and *P. brutia* Ten. In: Nee'man, G.T.L. (Ed.), Ecology, Biogeography and Management of *Pinus Halepensis* and *P. Brutia* Forest Ecosystems in the Mediterranean Basin. Backhuys Publishers, Leiden, The Netherlands, pp. 51–65.

Schiller, G., Ungar, E.D., Genizi, A., 2005. Is tree fate written in its tree rings? Characterization of trees in Kramim forest following the 1998/99 dry winter. Yaar, 18–25 (In Hebrew).
Schiller, G., Ungar, E.D., Cohen, S., Moshe, Y., Atzmon, N., 2009. Aspect effect on transpiration of *Pinus halepensis* in Yatir forest. Yaar 11, 14–19 (In Hebrew).
Schwinning, S., Sala, O.E., Loik, M.E., Ehleringer, J.R., 2004. Thresholds, memory, and seasonality: understanding pulse dynamics in arid/semi-arid ecosystems. Oecologia 141, 191–193.
Shaw, J.D., Steed, B.E., DeBlander, L.T., 2005. Forest Inventory and Analysis (FIA) annual inventory answers the question: what is happening to pinyon-juniper woodlands? J. For. 103, 280–285.
Song, C., Woodcock, C.E., Seto, K.C., Lenney, M.P., Macomber, S.A., 2001. Classification and change detection using Landsat TM data: when and how to correct atmospheric effects? Rem. Sens. Environ. 75, 230–244.
Tucker, C.J., 1979. Red and photographic infrared linear combinations for monitoring vegetation. Rem. Sens. Environ. 8, 127–150.
Ungar, E.D., Rotenberg, E., Raz-Yaseef, N., Cohen, S., Yakir, D., Schiller, G., 2013. Transpiration and annual water balance of Aleppo pine in a semiarid region: implications for forest management. For. Ecol. Manage. 298, 39–51.
Verbyla, D., 2008. The greening and browning of Alaska based on 1982–2003 satellite data. Glob. Ecol. Biogeogr. 17, 547–555.
Vicente-Serrano, S.M., 2007. Evaluating the impact of drought using remote sensing in a Mediterranean, semi-arid region. Nat. Hazard. 40, 173–208.
Vicente-Serrano, S.M., Saz-Sanchez, M.A., Cuadrat, J.M., 2003. Comparative analysis of interpolation methods in the middle Ebro Valley (Spain): application to annual precipitation and temperature. Clim. Res. 24, 161–180.
Vicente-Serrano, S.M., Begueria, S., Lopez-Moreno, J.I., 2010a. A multiscalar drought index sensitive to global warming: the standardized precipitation evapotranspiration index. J. Clim. 23, 1696–1718.
Vicente-Serrano, S.M., Begueria, S., Lopez-Moreno, J.I., Angulo, M., El Kenawy, A., 2010b. A new global 0.5° Gridded Dataset (1901–2006) of a multiscalar drought index: comparison with current drought index datasets based on the palmer drought severity index. J. Hydrometeorol. 11, 1033–1043.
Vicente-Serrano, S.M., Lasanta, T., Gracia, C., 2010c. Aridification determines changes in forest growth in *Pinus halepensis* forests under semiarid Mediterranean climate conditions. Agric. For. Meteorol. 150, 614–628.
Vicente-Serrano, S.M., Gouveia, C., Camarero, J.J., Beguería, S., Trigo, R., López-Moreno, J.I., Azorín-Molina, C., Pasho, E., Lorenzo-Lacruz, J., Revuelto, J., Morán-Tejeda, E., Sanchez-Lorenzo, A., 2013. Response of vegetation to drought time-scales across global land biomes. Proc. Nat. Acad. Sci. USA 110, 52–57.
Vila, B., Vennetier, M., Ripert, C., Chandioux, O., Liang, E., Guibal, F., Torre, F., 2008. Has global change induced divergent trends in radial growth of *Pinus sylvestris* and *Pinus halepensis* at their bioclimatic limit? The example of the Sainte-Baume forest (south-east France). Ann. For. Sci. 65, 709p701–709p709.
Volcani, A., Karnieli, A., Svoray, T., 2005. The use of remote sensing and GIS for spatio-temporal analysis of the physiological state of a semi-arid forest with respect to drought years. For. Ecol. Manage. 215, 239–250.
Wang, X., Piao, S., Ciais, P., Li, J., Friedlingstein, P., Koven, C., Chen, A., 2011. Spring temperature change and its implication in the change of vegetation growth in North America from 1982 to 2006. Proc. Nat. Acad. Sci. USA 108, 1240–1245.
Yuhas, A.N., Scuderi, L.A., 2009. MODIS-derived NDVI characterisation of drought-induced evergreen Dieoff in Western North America. Geogr. Res. 47, 34–45.
Zavala, M.A., Espelta, J.M., Retana, J., 2000. Constraints and trade-offs in Mediterranean plant communities: the case of holm oak-Aleppo pine forests. Bot. Rev. 66, 119–149.
Zhu, W., Tian, H., Xu, X., Pan, Y., Chen, G., Lin, W., 2012. Extension of the growing season due to delayed autumn over mid and high latitudes in North America during 1982–2006. Glob. Ecol. Biogeogr. 21, 260–271.